Ion Transport in Zeolites

DOI: 10.1002/anie.200605049

Matrix Effect on Motional Coupling and Long-Range Transport of Cations in Zeolites**

*Edgar Jordan, Dirk Wilmer, and Hubert Koller**

Research on the underlying mechanisms of local ionic motion and long-range transport in porous solid electrolytes is driven by the quest for the better control over ion conductivities. State-of-the-art approaches focus on the influences of defects and local cation-jump activation.[1–3] In addition, the number density of charge carriers that contribute to the conduction process is important. In principle, a particular cation conductivity can be achieved when all cations contribute to a similar extent or when a small number of cations are relatively fast. We describe here the impact of the topological environment on the motional coupling of ions. Two zeolites that have the same chemical composition and local cation coordination but different long-range topologies were employed to investigate cation coupling and matrix effects on cation conductivity. Impedance and solid-state NMR spectroscopies were used to analyze the contributions of different cations to direct-current (dc) conductivities. This combination of methods can be used for investigations on other systems.

The aluminosilicate zeolites sodalite (SOD) and cancrinite (CAN) (Figure 1) are ideal model systems for the systematic investigation of the matrix influence on motional couplings. CAN has a hexagonal structure with one-dimensional 12-ring channels running along the crystallographic *c* axis. These channels are surrounded by stacked arrays of ε-cages ($6^5 4^6$ cages).[4,5] The SOD framework consists of a three-dimensional space-filling packing of β-cages ($6^8 4^6$ cages).[6] Extraframework cations are located over 6-ring windows ($Al_3Si_3O_6$ rings) in all voids of these microporous aluminosilicates, either with or without coordination of extraframework anions. While the SOD structure can be synthesized with or without additional extraframework anions, the CAN synthesis requires the use of anions, such as carbonate, sulfate, and chromate, which are located in the large 12-ring channels.[7–9] In our research reported here, we synthesized these two structures with the tetraoxo anions chromate and sulfate. As no more than four cations can be located in one SOD cage, an alternating cage filling results in SOD as a result of charge-compensation requirements: anion-filled cages ($|Na_4CrO_4|$) and anion-free cages ($|Na_4|$). Three cations of each cage compensate the charge of the aluminosilicate framework, and one in each cage neutralizes the divalent chromate anion. The situation differs in CAN: in each unit cell six cations and the chromate anion are located in the 12-ring channel, and two sodium cations are in the ε-cages. These scenarios are reflected in the two formulas: $|Na_6CrO_4||Na_2|[Al_6Si_6O_{24}]$-CAN, and $|Na_4CrO_4||Na_4|[Al_6Si_6O_{24}]$-SOD.

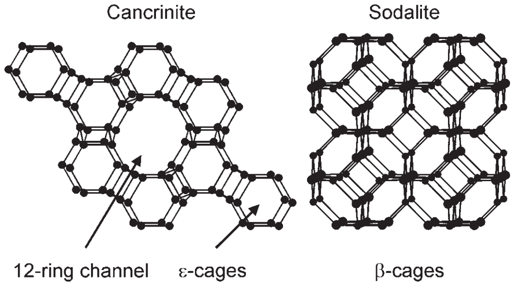

Figure 1. Framework structures of CAN and SOD. Filled black circles are tetrahedral Si or Al centers, and oxygen atoms are omitted.

It has been shown by ^{23}Na solid-state NMR and force-field calculations that cation–anion interactions reduce the activation barrier of local cation jumps.[10] In this work, investigations are extended to long-range conductivity. Special attention was given to the possible influence of the matrix topology. The number of cations in topologically different environments contributing to dc conductivity was analyzed by combining information from impedance and NMR spectroscopy. First, the jump rates for dc conductivity were determined from conductivity data by two independent methods.[11] Figure 2a shows the frequency-dependent conductivities of chromate SOD at various temperatures. The jump rates were estimated from the frequency range at which the conductivity leaves the dc plateau (method 1). For example, a value of 200 kHz is obtained at 573 K.

Second, jump rates were calculated from an analytical equation that combines the Nernst–Einstein equation with a random-walk model for cation motion (method 2) [Eq. (1) with the activation energy E_a and the observation frequency Γ_0]. The observation frequency corresponds to the preexponential factor A_0 of the Arrhenius representation of dc conductivities [Eq. (2)].

$$\Gamma = \Gamma_0 \exp(-E_a/RT) \quad (1)$$

$$A_0 = \Gamma_0 \frac{N_V q^2 x_0^2}{2Dk} \quad (2)$$

N_V is the number density of mobile ions, q the charge, D the dimensionality of the cation transport, and x_0 the average

---

[*] Dr. E. Jordan, Priv.-Doz. Dr. D. Wilmer, Priv.-Doz. Dr. H. Koller
Institut für Physikalische Chemie
Westfälische Wilhelms-Universität
Corrensstrasse 36, 48149 Münster (Germany)
Fax: (+49) 251-832-3409
E-mail: hubert.koller@uni-muenster.de
Homepage: http://www.uni-muenster.de/chemie.pc/koller

[**] Financial support by the Deutsche Forschungsgemeinschaft (SFB 458) is gratefully acknowledged.

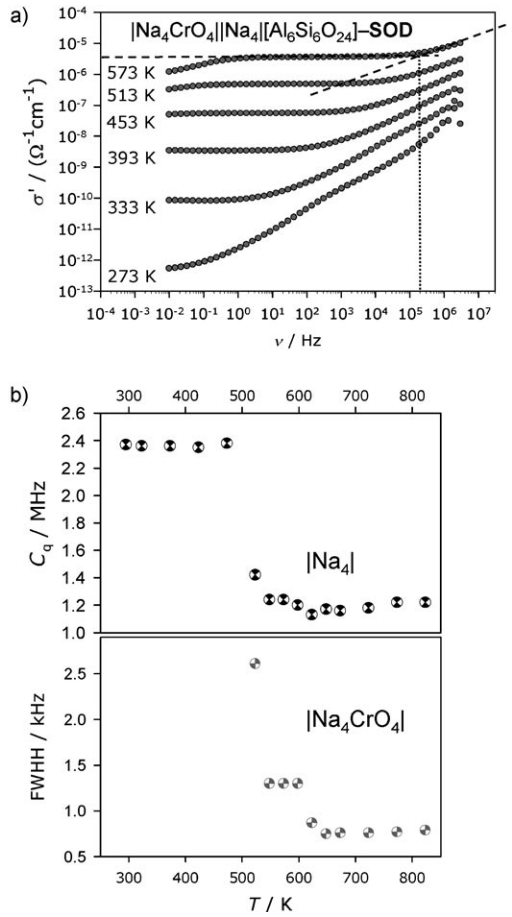

Figure 2. a) Frequency-dependent conductivities and b) dynamic ^{23}Na solid-state NMR data of chromate SOD. The estimation of jump rates is indicated for 573 K. The dynamic NMR information is obtained from the temperature dependence of the quadrupole coupling constant C_q for cations in the anion-free cage or from the values of full width at half-height FWHH in the cage with chromate.

jump distance. A_0 and E_a can be obtained easily from the Arrhenius analysis of dc conductivities. The average jump distance, 0.325 nm, was adopted from local jump models studied by force-field calculations.[10] For the number density of mobile ions N_V and the dimensionality D different scenarios were tested, and their consistency with the first method and NMR data was evaluated.

For chromate SOD, an activation energy E_a of (73.3 ± 0.4) kJ mol^{-1} and a preexponential factor A_0 of (4690 ± 630) Ω^{-1}cm^{-1}K were obtained. The jump-rate analysis according to Equation (1) yields a value of 270 kHz at 573 K, when all sodium cations participate in a three-dimensional conduction process. This value is in good agreement with the experimental estimation from the first method at the same temperature. This result shows that all cations contribute to the conduction process; that is, a considerably faster motion by a smaller number of cations leading to the same conductivity can be ruled out. Figure 2b shows the quadrupole coupling constants C_q and the full width at half-height values (FWHH) from static ^{23}Na NMR spectra of sodium cations in anion-free and anion-loaded SOD cages, respectively. The C_q values from these static NMR data are, within an estimated simulation error of 0.2 MHz, in excellent agreement with the results from MAS NMR analysis.[10] An analysis of C_q for anion-filled cages was not possible from the static NMR data owing to relatively small linewidths. Both lines exhibit a dynamic narrowing in the temperature range between 500 and 600 K. Line narrowing is observed when the jump rates are at least as high as the static NMR linewidth. From Figure 2a it can be estimated that the required jump rates of 8 kHz, that is, the linewidth of the broader component, for NMR line narrowing of anion-free cages are reached above ≈500 K. This temperature is in excellent agreement with the temperature range in which the line narrowing occurs in the NMR data (Figure 2b). This ensures that both methods, NMR and conductivity measurements, probe the same dynamic time scale for this temperature range, and all sodium cations must participate in a cooperative motional scenario. In other words, chromate sodalite is a dynamically (and topologically) homogeneous system.

A similar analysis of chromate CAN results in a different scenario (Figure 3). While the exchange process between two sites in the large 12-ring channel ($|Na_6CrO_4|$) is fully activated at 470 K (Figure 3b, top, MAS NMR data), a local two-site jump in the ε-cages ($|Na_2|$) requires a considerably higher temperature (750 K) to be fully developed (Figure 3b, bottom, static NMR data).[10] These cation motions are clearly decoupled. The estimated slowest jump rate at 573 K from frequency-dependent conductivities (Figure 3a) is approximately 2.0 kHz (method 1). This jump rate is just fast enough for the dynamic averaging observed by ^{23}Na MAS NMR spectroscopy in the 12-ring channels (components 1+2, averaged signal 4), and it is more than one order of magnitude too slow for the narrowing of the ^{23}Na NMR linewidth for the cations in the ε-cages (component 3). Hence, jump-rate analysis from conductivity data using Equation (1) (method 2) yields a value of 2.8 kHz which is in good agreement with method 1, when only cations in the 12-ring channels are considered in a one-dimensional conduction process with $E_a = (89.2 \pm 1.0)$ kJ mol^{-1} and $A_0 = (4746 \pm 970)$ Ω^{-1}cm^{-1}K. These observations lead to the conclusion that jump processes for cations in the two different voids in CAN are decoupled, and only the cations in the large channels contribute to dc conductivity at 573 K. Chromate CAN shows a rather low dc plateau. SOD is a three-dimensional conductor and has dc conductivities and jump rates that are higher by two orders of magnitude.

Replacing chromate by sulfate results in a somewhat different situation. Sulfate CAN is a better ion conductor than sulfate SOD, but the differences are not as pronounced as for the chromate zeolites. The jump rate in CAN from method 1 is 20 kHz at 573 K, and method 2 yields 27 kHz with $E_a = (74.8 \pm 0.4)$ kJ mol^{-1} and $A_0 = (2191 \pm 380)$ Ω^{-1}cm^{-1}K. Again, only cations in the 12-ring channels were considered for a one-dimensional conductor. The dimensionality is again consistent with the decoupled motion observed in the NMR data. Sulfate SOD shows a slightly lower dc conductivity with an activation energy of (80.5 ± 0.6) kJ mol^{-1} and $A_0 = (141 \pm 28)$ Ω^{-1}cm^{-1}K. Jump rates at 573 K are 3 kHz as determined by method 1 and 1.9 kHz by method 2.

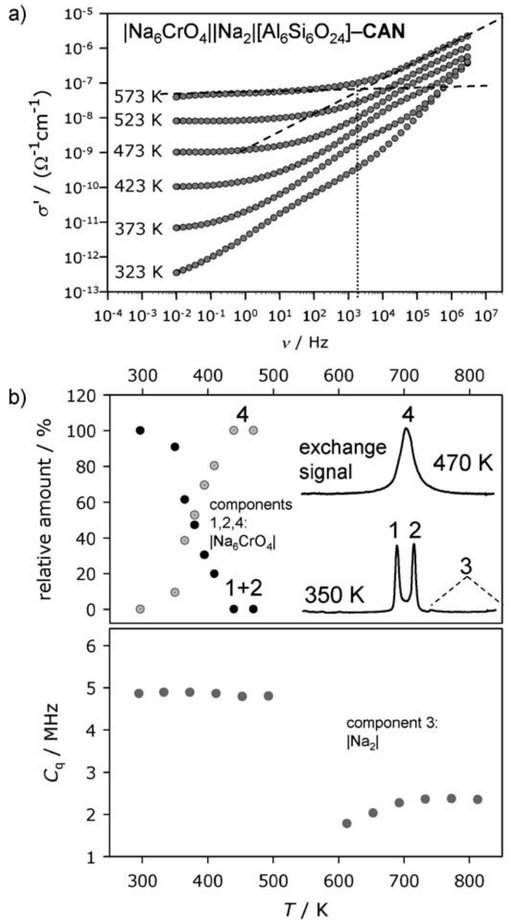

Figure 3. a) Frequency-dependent conductivities and b) dynamic ^{23}Na solid-state NMR data of chromate CAN. The estimation of jump rates is indicated for 573 K in (a). The dynamic NMR information is obtained from the quadrupole coupling constant C_q of cations in the anion-free cage (component 3), or from the relative intensities of the two separate lines and the exchange signal in the 12-ring channel with chromate (components 1,2,4).

The differences between the sulfate and chromate zeolites are mainly explained by the different activation energies. Chromate has a higher ionicity than sulfate. This factor is suggested to govern the differences in the observed conductivities. Sodium cations move through the CAN 12-ring channels in a one-dimensional mechanism. The higher ionicity of chromate relative to sulfate disfavors cation jumps since the transition state along the electrostatic potential surface is higher. The electrostatics of the anions plays a less important role in the SOD structure, because the cations penetrate through the three-dimensional network, including anion-free cages. Here, the transition state of cation movement is characterized by higher coordination during ring passage between different cages, whereas the motion within the CAN channels involves a reduction of coordination, which is associated with a higher activation barrier. Anion reorientation in the chromate structures may provide an additional promotion of local cation movement to overcome part of this latter barrier. ^{17}O NMR analyses show that chromate anions are subject to fast isotropic reorientation, whereas sulfate ions are immobile in both structures.[10] The anion dynamics for the chromate samples are suggested to contribute to the higher preexponential factor A_0 which is an entropic indicator.[3] However, a dynamic coupling of anion and cation motion on the same time scale in the sense of a paddle wheel was not observed by NMR spectroscopy.

The study clearly shows that all sodium cations in the topologically homogeneous SOD structure undergo cooperative motion, irrespective of the presence or absence of an interacting anion in the cage. No such coupling exists between cation migration in CAN channels and local jumps in small cages. Thus, CAN is a one-dimensional conductor in the investigated temperature range. A combination of frequency-dependent conductivity measurements and solid-state NMR spectroscopy was crucial for the key conclusions on void-specific ionic motion. While the NMR lineshape data typically yield dynamic information on the local scale up to about 1 nm, the dc plateau of conductivity spectra probes long-range transport. The latter does not necessarily require a single charge carrier (that is, a particle or a hole) traveling over a large distance. Rather, a chain mechanism that involves many particles is also feasible in which the single species contributes only on a short distance to the long-range process. Both the long-range journey of a single particle (or hole) and such collective displacement mechanisms might be hindered by transport resistance. The lack of sufficient vacancies is a typical transport resistance for ion conduction. Additionally, local defects or stacking faults of the crystals could also hinder long-range transport, as was previously suggested for the diffusion of alkanes in MFI-type zeolites by a combination of NMR spectroscopy and quasi-elastic neutron scattering.[12]

Usually, such orientation-specific information on the diffusion of charge carriers can be obtained only by conductivity measurements on single crystals,[13] which are often not available. All cations in SOD participate in dc conductivity, although they are located in cages with different electrostatic situations, with and without anion filling. We suggest that the motional decoupling in CAN is a result of the larger distance between cation sites of the two voids. These findings on two model frameworks with the same chemical composition will provide a basis for future theoretical and experimental investigations of the underlying mechanisms and influences of electrostatic and structural environments on ion conduction. Such studies will be useful to improve cation conductivities of zeolites by design. The current performances in the dc conductivities are some orders of magnitude too low for fast ion conductors. However, they are interesting for applications, such as sensor materials, where the porosity of an electrolyte material with moderate conductivity is crucial.

Received: December 14, 2006
Published online: March 27, 2007

Keywords: impedance spectroscopy · ionic conductivity · NMR spectroscopy · zeolites

---

[1] M. E. Franke, M. Sierka, U. Simon, J. Sauer, *Phys. Chem. Chem. Phys.* **2002**, *4*, 5207–5216.

[2] M. E. Franke, U. Simon, R. Moos, A. Knezevic, R. Müller, C. Plog, *Phys. Chem. Chem. Phys.* **2003**, *5*, 5195 – 5198.
[3] T. C. Wei, H. W. Hillhouse, *J. Phys. Chem. B* **2006**, *110*, 13728 – 13733.
[4] H. D. Grundy, I. Hassan, *Can. Mineral.* **1982**, *20*, 239 – 251.
[5] H. D. Grundy, I. Hassan, *Can. Mineral.* **1984**, *22*, 333 – 340.
[6] J. Löns, H. Schulz, *Acta Crystallogr.* **1967**, *23*, 434 – 436.
[7] R. M. Barrer, J. F. Cole, H. Sticher, *J. Chem. Soc.* **1968**, 2475 – 2785.
[8] R. M. Barrer, J. F. Cole, H. Villiger, *J. Chem. Soc. A* **1970**, 1523 – 1531.
[9] R. M. Barrer, J. F. Cole, *J. Chem. Soc.* **1970**, 1516 – 1523.
[10] E. Jordan, R. G. Bell, D. Wilmer, H. Koller, *J. Am. Chem. Soc.* **2006**, *128*, 558 – 567.
[11] “Concept of Mismatch and Relaxation for Self-Diffusion and Conductivity in Ionic Materials with Disordered Structures”: K. Funke, C. Cramer, D. Wilmer in *Diffusion in Condensed Matter* (Eds.: P. Heitjans, J. Kärger), Springer, Berlin, **2005**.
[12] H. Jobic, W. Schmidt, C. B. Krause, J. Kärger, *Microporous Mesoporous Mater.* **2006**, *90*, 299 – 306.
[13] N. Yamamoto, T. Okubo, *Microporous Mesoporous Mater.* **2000**, *40*, 283 – 288.